ASEAN Journal of Chemical Engineering 2025, Vol. 25, No. 2, 286–297

Influence of Chitosan Concentration on the Properties of Electrospun Methanol-crosslinked Chitosan/PVA Nanofibers

Nurul Aina Munirah Binti Ahmadi [1]
Noor Fauziyah Binti Ishak [*,1]
Mohd Reusmaazran Bin Yusof [2]
[1] *School of Chemical Engineering, College of Engineering, Universiti Teknologi MARA, 40450 Shah Alam, Selangor, Malaysia*
[2] *Material Technology Group, Industrial Technology Division, Malaysian Nuclear Agency*
*e-mail: noorfauziyah@uitm.edu.my

Submitted 24 September 2024 *Revised* 11 April 2025 *Accepted* 19 April 2025

Abstract. Polymers nanofibers are of great interest due to the growing need for advanced materials to be used in biomedical applications. This research seeks to assess how the chitosan (CS) concentration affects the electrospun methanol-crosslinked CS/polyvinyl alcohol (PVA) nanofibers' characteristics. Polymer solution compositions containing 10%, 20%, and 30% CS were prepared and electrospun into nanofibers and then crosslinked with methanol to increase their stability. The nanofibers formed were characterized by their morphology, wettability, and crystallographic structure. According to the FESEM, the 20% CS had the largest diameter range (180-240 nm), while the smallest diameter range (120-160 nm) was noticed in the 10% CS. Nonetheless, the rats with 20% CS had the fewest beads during electrospinning. The analysis of WCA shows that the nanofibers had good wettability, as they all exhibited 31° as the lowest contact angle for the 20% CS. From the XRD, the nanofibers fabricated with 10% CS exhibited the highest peak intensity, which implies a more crystalline structure than the rest. However, the 20% CS nanofibers had a more amorphous structure, which could be useful in biomedical applications like wound dressing. The study demonstrates that the concentration of chitosan and methanol crosslinking significantly influences the electrospun nanofibers's morphological, hydrophilic, and structural aspects.

Keywords: Chitosan, Composite Fibers, Crosslinking, Electrospinning, Polyvinyl Alcohol

INTRODUCTION

Skin wounds can occur due to surgical incisions, scrapes, pressure ulcers (bed sores), or other types of injury (Nancy *et al*., 2022). Wound care products are available to enhance healing and prevent infections. These products include absorbent dressings and moisture-retaining hydrogels, seaweed-based alginates for fluid absorption, and conformable hydrocolloid dressings (Shah *et al*., 2019). The best dressing should be flexible for ease of movement and stable enough to protect the wound. Materials that can degrade naturally (biodegradable) are also preferable (Barleany *et al*., 2023). Due to the recent advances in biomaterials and hydrogels, this has presented new dressings with exciting prospects. These advanced dressings are not only designed to manage the wound but may also stimulate healing. They can create a moist atmosphere,

DOI: 10.22146/ajche.16579

minimize inflammation, and even release cells or growth factors to fast-track the healing process (Farahani & Shafiee, 2021). Recent research by Das and Mazumder (2023) emphasizes the potential of incorporating bioactive agents into these materials. This method can enhance healing by reducing inflammation and encouraging tissue regeneration, providing a more proactive approach to wound management (Das & Mazumder, 2023).

Hydrogels, three-dimensional networks made by linking long chains of water-absorbent (hydrophilic) polymers (Waqar *et al*., 2025), resemble small sponges that retain significant water within their mesh. Such capabilities simulate several living tissue properties because their natural extracellular matrix surrounding cells closely resembles some of these characteristics (Ho *et al*., 2022). Hydrogels can generally be categorized into two major types based on the origin of the source materials, which are natural and synthetic. Natural hydrogels originate from native polymers such as chitosan, sodium alginate, collagen, and sodium hyaluronate (Kaczmarek *et al*., 2020). Among these, chitosan (CS), a chitin-derived polysaccharide, is a critical focus because of its useful applications in wound healing. CS-based preparations have shown the ability to hasten hemostasis, inhibit microbial infections, and boost cell proliferation at critical stages of cutaneous regeneration (Feng *et al*., 2021). However, poor solubility and stability, especially in aqueous media, limit the CS preparation, affecting its processability and performance (Pellis *et al*., 2022).

To overcome these limitations, CS is commonly blended with synthetic polymers like polyvinyl alcohol (PVA) (H. Zhang et al., 2022). Thus, due to its high tensile strength, biocompatibility, and outstanding water retention capabilities (López de Armentia Hernández, 2022), blended CS/PVA hydrogels and nanofibers have been studied to capture the advantages of both materials. Still, several challenges exist (Hong *et al*., 2022). Various previous studies have employed conventional crosslinking agents like glutaraldehyde, which are cytotoxic, limiting the biomedical applicability of the formed fibers (Xu *et al*., 2023). Furthermore, minimal focus has been on optimizing CS concentration and its direct effect on nanofiber morphology, hydrophilicity, and crystallinity. These are critical parameters for designing wound dressing materials with mechanical and biological characteristics (Hernandez & Woodrow, 2022).

Another important gap in the literature is the type of crosslinking technique used to enhance the performance of CS/PVA electrospun nanofibers. While chemical crosslinkers like glutaraldehyde have been widely used to enhance mechanical stability (Hu *et al*., 2020), their toxicity raises concerns for biomedical use. Methanol seems safer and less toxic than chemical crosslinkers and is a simple approach that has not been fully exploited in this context (Nguyen *et al*., 2020). Methanol treatment has been demonstrated to accomplish physical crosslinking between polymer chains by inducing hydrogen bonding and chain rearrangements, subsequently improving structural stability and water resistivity for electrospun fibers without reactive chemical residues (Rianjanu *et al*., 2018). Such favorable effects and simplicity of application imply that methanol crosslinking is an essential method to enhance functional properties for CS/PVA nanofibers in biomedical applications that require biocompatibility.

This study recognizes these concerns and

seeks to fill the gap by determining how varying chitosan concentrations (10%, 20%, and 30%) affect morphology, wettability, and crystallinity in electrospun CS/PVA nanofibers crosslinked using methanol. This work aims to synthesize optimized nanofiber structures with worthwhile physical and chemical properties for wound healing applications by providing methanol as a new physical crosslinker and the systematic effect of CS concentration.

The nanofibers synthesized will be characterized by field emission scanning electron microscopy (FESEM) to evaluate diameter and morphology. Also, water contact angle (WCA) analysis and X-ray diffraction (XRD) will be done to assess the hydrophilicity and crystalline features, respectively. Such detailed evaluation will obtain adequate information on the methanol-crosslinked CS/PVA nanofibers' nanostructure with varying CS content. The results will provide insights into modifying nanofiber functionality while eliminating previous drawbacks associated with poor solubility, cytotoxic crosslinkers, and unsatisfactory fiber homogeneity.

MATERIALS AND METHODS

Materials

All salts and reagents were analytical grade. All solutions were prepared using Milli-Q water with a resistivity of 18.0 MΩ. Poly (vinyl alcohol) (PVA) in powder form (MW = 146,000–186,000 g/mol, 98–99% hydrolyzed), chitosan solution (1% in 1% acetic acid), medium molecular weight (MW = 161,000 g/mol), and methanol were purchased from Sigma-Aldrich Chemical (Malaysia).

Polymer Solution Preparation

Polymer solutions with different CS concentrations were prepared as follows. First, 0.7 g of PVA powder was weighed using an analytical balance and placed in three beakers to obtain a 14% (w/v) of the PVA solution. Distilled water was added, and each beaker was heated at 80°C with magnetic stirring for 1 h using a hot plate magnetic stirrer. This was done until the PVA was completely dissolved, yielding a clear PVA solution. Then, CS was added to the PVA solutions to get the required concentrations. 0.5 mL of CS solution (1% in 1% acetic acid) and 0.5 mL of methanol were injected into the PVA solution while stirring consistently to improve the crosslinking process to obtain a 10% (w/w) CS/PVA solution. The mixture was then sealed with parafilm and stirred overnight at room temperature. To obtain 20% and 30% (w/w) CS/PVA solutions, 1.0 mL and 1.5 mL of CS solution were added to the PVA solution, and stirred overnight, following the same procedures as the 10% solution.

Electrospinning Process

The electrospinning technique was employed to fabricate nanofibers using a syringe pump machine, as shown in Figure 1. A polymer solution was held in a 1 mL syringe while the syringe pump machine assisted in the fabrication of the polymer. The needle tip diameter was set to 25 nm, and the syringe size had a diameter of 25 cm. The distance between the syringe and the collector (an aluminum foil-covered surface) was 16 cm. A voltmeter reading of 15 volts was connected to the needle tip and the collector. To achieve a dense layering of nanofibers, 2 mL of the polymer solution was used from the syringe during fabrication. The relative humidity was controlled between 50 and 60% at room temperature. Throughout the electrospinning

process, the voltage and flow rate were kept constant at 17.5kV and 0.003ml/h of different polymer solutions with varying amounts of CS.

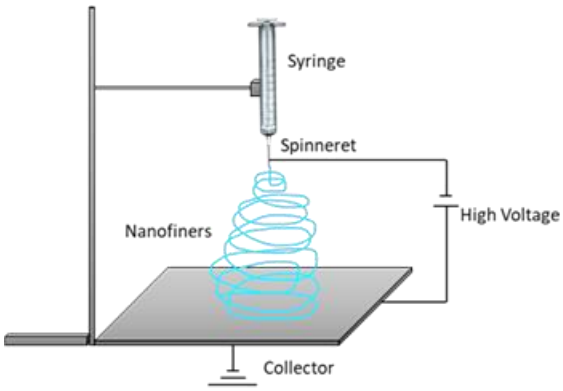

Fig. 1: The setup of electrospinning process

Sample Characterization

The produced nanofibers were gently detached from the aluminum foil collector and cut into 2x2 cm square pieces, which were stored in labeled zip-lock plastic bags. This ensured the nanofibers were ready for further examination across various parameters, allowing for intensive evaluation of their properties. Physical description tests helped identify the kind of material being dealt with, whereas chemical property evaluation provided insight into the safety and potential hazards associated with the nanofibers. This is essential for determining their suitability for use and potential risks to individuals who may contact them directly or indirectly.

The CS/PVA nanofibers were comprehensively chemically and physically characterized through various analytical techniques. Morphological evaluation was done using Field Emission Scanning Electron Microscopy (FESEM, Zeiss Model Supra VP35, Germany) to analyze the nanofiber structure. The dried samples, 2x2 cm in size, were sputter-coated with gold for 40 s and operated at an accelerating voltage of 15 kV. The mean diameter of the CS/PVA nanofibers was measured by analyzing the FESEM images using Nano Measurer software. Water Contact Angle (WCA) analysis (Theta Lite-100, Biolin Scientific, Finland) was used to investigate the nanofibers' hydrophilicity. X-ray Diffraction (XRD) analysis (Bruker, Model AXS D8, Germany) was conducted to establish the crystallographic structure within the nanofibers, operated at 50 kV and 200 mA using nickel-filtered Cu Kα radiation.

RESULTS AND DISCUSSION

FESEM Analysis

Using Field Emission Scanning Electron Microscopy (FESEM), the nanofiber morphology was assessed, as depicted in Figures 2(a), 2(b), and 2(c). The images show nanofiber structures and diameters differ depending on PVA's chitosan (CS) concentration. A nanofiber fabricated with 30% CS in 14% PVA-formed beads implies an irregular nanofiber morphology to some extent. The 20% CS nanofibers formed with minimal bead formation, implying uniformity, and beads were absent within the nanofiber structure. The nanofibers made with only 10% CS had beads. This is often the case when the solution's concentration is low, and the sol-gel viscoelastic force is insufficient to resist the repulsive forces of charge. This scenario results in polymer drops forming on the nanofibers, compromising the nanofibers' overall properties (Abdillah et al., 2022).

The study concluded that while polymers exhibit low resistance at low viscosity, surface tension significantly determines the final morphology. High surface tensions can lead to polymer drops rather than unique nanofibers. Bead formation must be present on the produced nanofibers (SIRIN *et al.*, 2013). The bead

formation reduces the surface area of the nanofibers by a larger extent, adversely affecting the performance of nanomaterials. Nanofibers with beads are often regarded as of poor quality, and electrospinning parameters are always adjusted to eliminate the beads to ensure high-quality nanofibers with acceptable surface area and morphology (Toriello et al., 2020a).

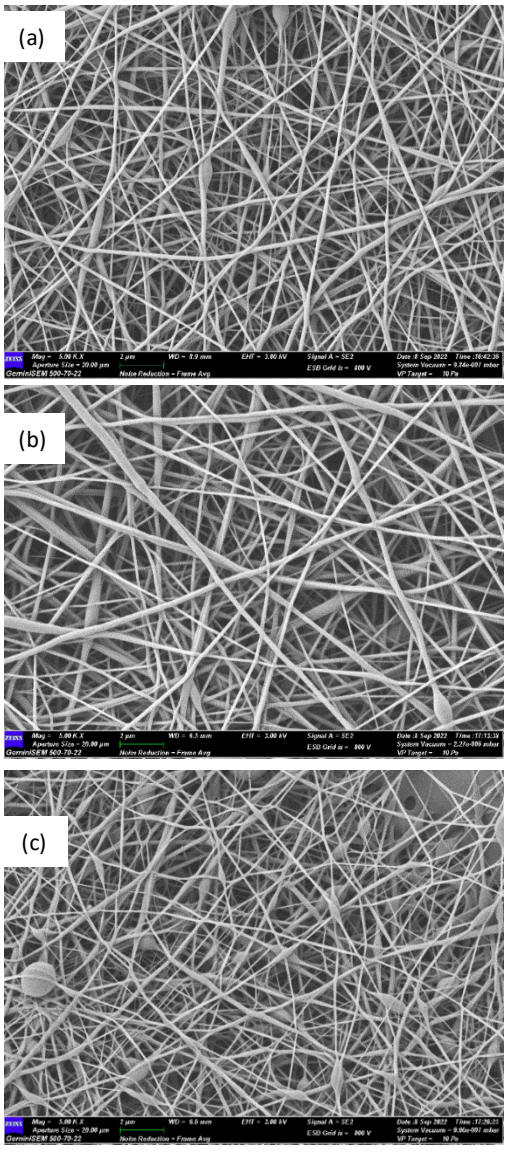

Fig. 2: Surface morphology using FESEM at 5000x magnification for (a) 30% CS, (b) 20% CS, and (c) 10% CS nanofibers.

Bead-free nanofibers, like wound dressings, are preferred in biomedical applications like wound dressings since they offer continuous structures that enhance cell attachment, nutrient transfer, and controlled drug release. Beads can create weak points, disrupt the fiber network, impede wound healing, and reduce mechanical stability (Yang *et al*., 2022). Hence, bead minimization is crucial to ensure such nanofiber-based biomaterials' structural integrity and functionality. The 20% CS formulation has a smooth and homogeneous morphology that demonstrates its applicability in biomedical, providing reasonable surface area and consistency.

In addition, the nanofiber diameters gave valid interpretations based on the relationship in varied concentrations. The 20% CS nanofibers had the widest range of diameters, ranging from 180-240 nm, as shown in Figures 3(a), 3(b), and 3(c). It may be attributed to increased polymer concentration, which causes increased polymer chain entanglements (Bobbili & Milner, 2020). This phenomenon results in thicker injected polymer from the syringe and, thus, high nanofiber diameters in the grounded collector surfaces. The diameter range for the 10% CS was slightly lower than that of the 20% with a range of 120-160 nm, while for the 30% CS, it was 150-170 nm. Polymer chain entanglements and the corresponding nanofiber morphology could explain the disparity in diameter.

A conclusion drawn from the morphological inspection and diametrical analyses is that the most appropriate percentage composition is 20% CS. Its attribute of producing fewer beads resulted in a high average diameter and nanofibers' homogeneity, which makes them appealing composites for any use. Thus, these findings highlight the necessity of precise formulation to achieve the composite properties desired.

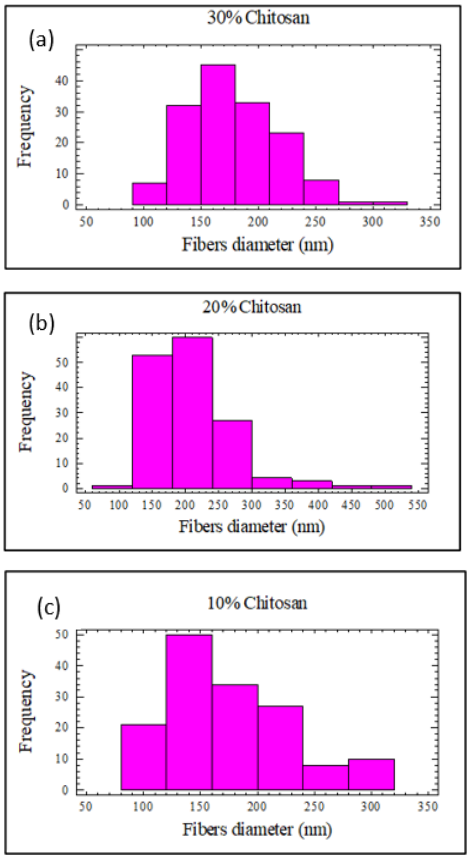

Fig. 3: Estimated diameter of nanofibers using FESEM for (a) 30% CS, (b) 20% CS and (c) 10% CS in PVA solution.

These results align with earlier research, which showed that optimal chitosan concentration reduces bead formation and favors evenly spread fibers. Anisiei *et al.* (2023) demonstrated that a chitosan concentration of 15–25% produced the most homogeneous nanofibers with the fewest defects, underscoring the essential involvement of polymer entanglement in controlling morphology (Anisiei *et al.*, 2023).

WCA Analysis

The wetting ability and surface energy properties of CS/PVA nanofibers were measured, as surface energy is a direct measure of the contact angle. Smaller angles signify higher surface energies, which promote better wettability (Huhtamäki *et al.*, 2018). The following part seeks to assess the data in Figure 4 on WCA measurements obtained from different percentages of CS incorporated into a 14% PVA matrix. In this study, the 10% CS nanofibers show contact angles ranging from 42.60° to 42.84°, taken as the average value of 42.74°, as depicted in Figure 4(c).

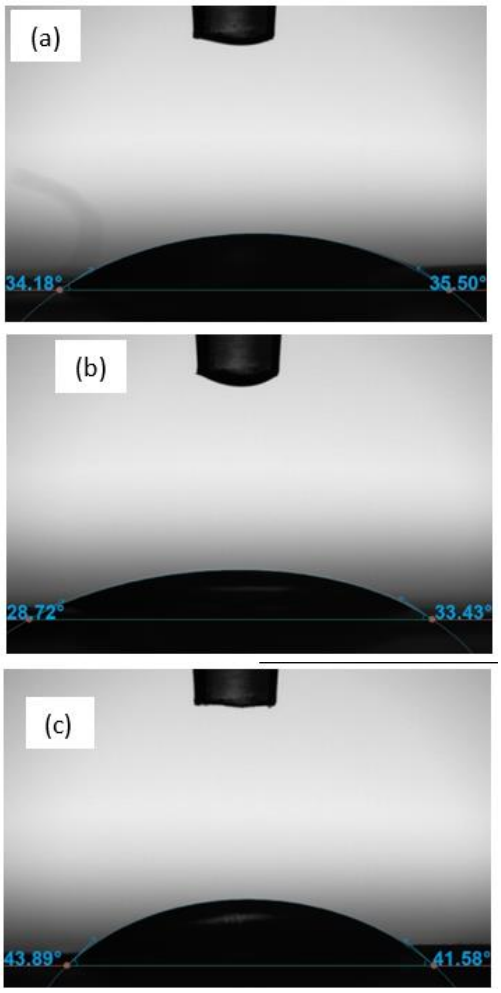

Fig. 4: WCA of nanofibers for (a) 30% CS, (b) 20% CS, and (c) 10% CS in PVA solution.

This relatively high contact angle suggests that these nanofibers are less wetted and have lower surface energy (Hou et al., 2018). On the other hand, at 20% CS nanofiber, it could be observed that it was a relatively small variation in the range, with a minimum of 30.80° and a maximum of 31.22°, giving an average value of 31.00°. The small

value indicates that the nanofiber with 20% CS has a higher surface energy, hence better wettability. This increase in wettability is advantageous in most applications because it ensures easy interaction of the nanofibers and other substances (Toriello et al., 2020b). However, at 30% CS, the WCA values fluctuate between 34.69° and 35.14°, thus recording the highest average of 34.70°. Despite measuring neither too high nor too low, these nanofibers can be considered moderate in surface energies.

The trend of WCA results reveals a clear relation with different CS concentrations. The contact angle reduces as the CS content progressively increases from 10% to 30%. The nanofiber from 20% CS in the 14% PVA matrix has the lowest contact angle, thus indicating minimal bead formation. This implies a uniformity of structure and absence of beads in the nanofibers, as shown by the FESEM images. Hence, the 20% CS formulation best balances surface energy and wettability. Thus, it is ideally suited for such wound dressing.

Improved wettability is associated with greater fluid absorption and enhanced material-tissue interaction in wound-healing situations. The 20% CS nanofibers had a lower contact angle, implying higher hydrophilicity, enabling the fibers to absorb wound exudates. This property is critical to maintaining a moist wound environment and is instrumental in faster re-epithelialization and tissue repair (H. Zhang et al., 2021). In addition, improved surface wettability enhances the nanofiber mat's capacity to adhere to biological tissue surfaces, which allows better contact, eliminating dead space and facilitating cell migration and proliferation (Kurusu & Demarquette, 2019). Therefore, nanofibers' excellent wettability signifies improved surface energy and clinical performance as wound dressing materials.

XRD Analysis

The crystal composition and atomic arrangement of CS/PVA nanofibers can be studied through X-ray diffraction (XRD). With this technique, various phases and properties found in nanostructured materials embedded in the nanofibers can be identified. Figure 5 displays XRD patterns at different CS concentrations (10%, 20%, and 30% concerning PVA concentration, which is 14 wt%). The peaks were observed at $2\theta = 20°$ and exhibit variable intensities in these patterns, where the highest peak intensity is recorded for 10% CS, followed by 30% CS, and the lowest intensity for 20% CS. The result supports the findings of Bharati *et al.* (2021), which indicated that blending CS with PVA reduced its crystallinity (Bharati *et al.*, 2021). Additionally, results from Abbas *et al.* (2020) validated that decreased crystallinity improves nanofiber swelling and flexibility (Abbas *et al.*, 2020), which are advantageous in wound healing since these features are important in preparing materials that require adaptability and high absorption.

The CS/PVA nanofibers exhibit a considerably reduced original peak of PVA at $2\theta = 20°$ in Figure 5(a). This indicates that the crystalline structure of PVA was altered upon blending with CS. The electrospinning process did not improve these nanofibers' crystallinity but hindered the evolution of a crystalline microstructure, thus creating a more amorphous one. The 20% CS/PVA nanofiber sample showed the weakest crystallinity peak, indicating this blend ratio since it appears to be the most amorphous. Furthermore, probably due to solvent entrapment in the polymer structure, the low crystallinity of the CS/PVA nanofibers may also be explained (Abbas *et al.*, 2020).

The position and intensity of the diffraction peaks give clues regarding the

crystal structure and properties of the nanofibers. Sharp peaks suggest large crystallites, while broad peaks reflect small crystallites (Raja *et al*., 2022). The XRD pattern of CS/PVA nanofibers reflects sharp and broad peaks, suggesting a blend of crystallite sizes. Larger crystals have a more ordered arrangement, yielding narrower peaks, while smaller crystals are less ordered, resulting in broader peaks. This indicates that some regions of the nanofibers contain predominantly large crystallites while others contain mainly smaller ones. The thicker lines correspond to larger average grain sizes, while the thinner lines correspond to smaller average grain sizes.

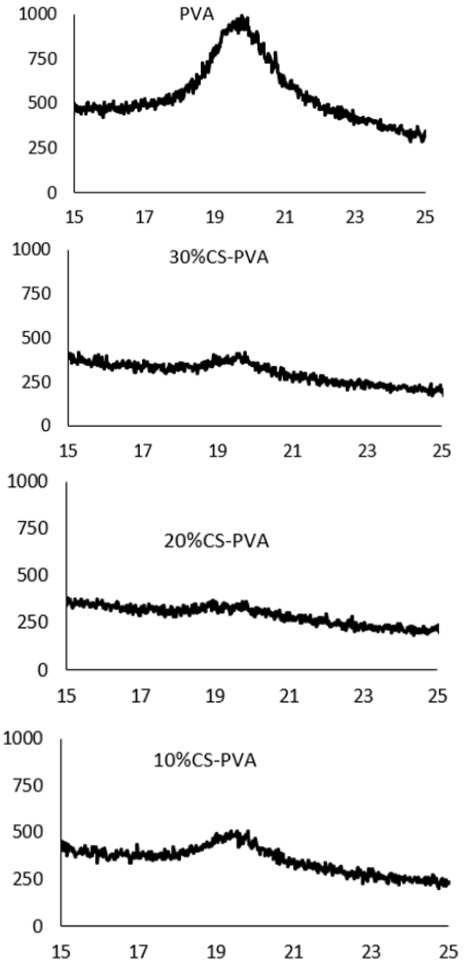

Fig. 5: XRD of (a) PVA and nanofibers for (b) 30% CS, (c) 20% CS, and (d) 10% CS in PVA solution.

The crystallinity of CS/PVA nanofibers is essential for their functionality as wound dressing. High crystallinity often improves the mechanical strength and stability of the nanofibers, thus supporting tissue regeneration (Han *et al*., 2021). However, the amorphous form shown most in the 20% CS formulation can also be desirable since it is a means to improve the flexibility and swelling capability of the nanofibers for better synergy with biological tissues. A balance between crystallinity and amorphousness in CS/PVA nanofibers will also affect their ability to absorb exudates and ensure a moist environment crucial for wound healing. The discussion above about the XRD of CS/PVA nanofibers concerning CS concentration is essential for understanding crystallinity in CS/PVA composite nanofibers, which has meaningful effects on their performance in biomedical applications.

Conversely, the 20% CS formulation's amorphous structure may deliver unique biomedical benefits. Increased amorphousness usually improves flexibility, elasticity, and swelling ability, facilitating biological tissue integration and wound site moisture retention (Sanjarnia *et al*., 2024). However, this flexibility improvement may compromise mechanical strength and long-term structural stability. Additionally, reduced crystallinity usually promotes higher degradation rates, which might be favorable or harmful depending on the advised period of use. A rate of quicker degradation is beneficial in temporary wound dressings, while long-term implant uses may need a more crystalline state (Niculescu & Grumezescu, 2022).

Thus, these data emphasize the need for an ideal trade-off between crystallinity and amorphousness to regulate nanofiber properties in varied biomedical uses. The 20%

CS/PVA formulation demonstrated a favorable compromise as it is structurally flexible and wettable while retaining adequate integrity for short- to medium-term wound healing applications.

CONCLUSIONS

In conclusion, the detailed characterization of CS/PVA nanofibers has provided insightful revelations about their properties and behaviors. The morphology study using FESEM showed that nanofibers produced using 20% CS in a 14% PVA matrix had the best structure as they exhibited minimal bead formation and the highest nanofiber diameter of 180-240 nm. Such uniformity and homogeneity are ideal for many applications. The WCA examination further supported the conclusion that the formulation with 20% CS provides the best balance between surface energy and wettability. The nanofibers composed of 20% CS had the lowest contact angle values, 30.78° - 31.22°, compared to the higher percentage formulations. A lower contact angle indicates higher surface energy and increased wettability. This improved wettability is advantageous for applications, including wound dressing, as it allows for better interaction between the nanofibers and other materials.

The XRD findings showed that the CS/PVA nanofibers possess a highly reduced original peak of PVA at $2\theta=20°$, implying that the crystalline structure of PVA was altered upon blending with CS. The weakest crystallinity peak of the sample 20% CS/PVA nanofiber was indicative that this sample, which had the highest percentage of CS incorporated into the blend, had the most significant impact on the crystalline structure of both polymers and produced the most amorphous morphology. Thus, the most appropriate percentage composition for CS in the PVA matrix is 20%. This is because it produces the fewest beads and results in higher average diameter and homogeneity within the nanofibers, making them composites for any application where these findings stress the proper formulation needed to achieve composite required properties.

RECOMMENDATIONS

Based on this study's results, some recommendations can be made for future research to support the advancement and implementation of CS/PVA electrospun nanofibers in medicine, especially in wound healing. First, although methanol was the physical crosslinking agent of choice due to its simplicity and capacity to generate favorable fiber morphology, future research should focus on optimizing the crosslinking conditions to ensure comprehensive removal of residual methanol and verify the biocompatibility of the fibers. Secondly, mechanical and degradation tests should be performed to assess the nanofibers' structural integrity and biodegradation rate. This is especially important as reduced crystallinity, while beneficial for flexibility and swelling, could negatively impact the long-term mechanical integrity. Furthermore, the excellent hydrophilicity and smooth morphology of the 20% CS formulation make it a viable candidate for wound dressing. However, biocompatibility assays, including cytotoxicity, antimicrobial activity, and cell proliferation tests, must be performed to confirm its clinical potential. Future research could also explore loading therapeutic agents or natural extracts into the nanofiber matrix to boost its bioactivity and wound-healing capabilities.

ACKNOWLEDGEMENT

The authors would like to acknowledge the School of Chemical Engineering, Universiti Teknologi MARA, Shah Alam, Selangor, Malaysia, and the Malaysian Nuclear Agency for the collaboration.

REFERENCES

Abbas, W. A., Sharafeldin, I. M., Omar, M. M., & Allam, N. K., 2020. "Novel mineralized electrospun chitosan/PVA/TiO_2 nanofibrous composites for potential biomedical applications: Computational and experimental insights." *Nanoscale Adv. 2(4)*, 1512–1522. https://doi.org/10.1039/d0na00042f.

Abdillah, U., Yazid, H., Ahmad, S., Makhtar, N., Zaubidah, S., Chen, R. S., & Syifa, N. H., 2022. "The effect of various electrospinning parameter and sol-gel concentration on morphology of silica and titania nanofibers." *IOP Conf. Ser. Mater. Sci. Eng. 1231(1),* 012012. https://doi.org/10.1088/1757-899X/1231/1/012012.

Anisiei, A., Oancea, F., & Marin, L., 2023. "Electrospinning of chitosan-based nanofibers: From design to prospective applications." *Rev. Chem. Eng. 39(1),* 31–70. https://doi.org/10.1515/revce-2021-0003.

Barleany, D. R., Jayanudin, J., Nasihin, N., Widiawati, M., Yulvianti, M., Sari, D. K., & Gunawan, A., 2023. "Hydrogel preparation from shrimp shell-based chitosan: The degree of crosslinking and swelling study." *ASEAN J. Chem. Eng. 23(1),* 28–39. https://doi.org/10.22146/ajche.73716

Bharati, D. C., Rawat, P., & Saroj, A. L., 2021. "Structural, thermal, and ion dynamics studies of PVA-CS-NaI-based biopolymer electrolyte films." *J. Solid State Electrochem. 25(6),* 1727–1741. https://doi.org/10.1007/s10008-021-04946-6.

Bobbili, S. V., & Milner, S. T., 2020. "Simulation study of entanglement in semiflexible polymer melts and solutions." *Macromolecules 53(10),* 3861–3872. https://doi.org/10.1021/acs.macromol.9b02681

Das, S., & Mazumder, A., 2023. "Recent advances in hydrogel-based drug delivery for wound healing therapy: A Systematic Review." *Allelopath. J. 59(2),* 197-206. https://doi.org/10.26651/allelo.j/2023-59-2-1442

Farahani, M., & Shafiee, A., 2021. "Wound healing: from passive to smart dressings." *Adv. Healthcare. Mater. 10(16)*, 2100477. https://doi.org/10.1002/adhm.202100477

Feng, P., Luo, Y., Ke, C., Qiu, H., Wang, W., Zhu, Y., Hou, R., Xu, L., & Wu, S., 2021. "Chitosan-based functional materials for skin wound repair: Mechanisms and applications." *Frontiers in bioengineering and biotechnology 9,* 650598. https://doi.org/10.3389/fbioe.2021.650598

Han, S., Nie, K., Li, J., Sun, Q., Wang, X., Li, X., & Li, Q., 2021. "3D electrospun nanofiber-based scaffolds: from preparations and properties to tissue regeneration applications." *Stem cells International 2021,* 8790143. https://doi.org/10.1155/2021/8790143

Hernandez, J. L., & Woodrow, K. A., 2022. "Medical applications of porous

biomaterials: Features of porosity and tissue-specific implications for biocompatibility." *Adv. Healthcare Mater. 11(9),* e2102087. https://doi.org/10.1002/adhm.202102087

Ho, T. C., Chang, C. C., Chan, H. P., Chung, T. W., Shu, C. W., Chuang, K. P., Duh, T. H., Yang, M. H., & Tyan, Y. C., 2022. "Hydrogels: Properties and applications in biomedicine." *Molecules 27(9)*, 2902. https://doi.org/10.3390/molecules27092902

Hong, Y., Lin, Z., Yang, Y., Jiang, T., Shang, J., & Luo, Z., 2022. "Biocompatible conductive hydrogels: applications in the field of biomedicine." *Int. J. Mol. Sci. 23(9)*, 4578. https://doi.org/10.3390/ijms23094578

Hu, D., Ren, Q., Li, Z., & Zhang, L., 2020. "Chitosan-based biomimetically mineralized composite materials in human hard tissue repair." *Molecules 25(20),* 4785. https://doi.org/10.3390/molecules25204785

Huhtamäki, T., Tian, X., Korhonen, J. T., & Ras, R. H. A., 2018. "Surface-wetting characterization using contact-angle measurements." *Nature Protocols 13(7),* 1521–1538. https://doi.org/10.1038/s41596-018-0003-z

Kaczmarek, B., Nadolna, K., & Owczarek, A., 2020. "The physical and chemical properties of hydrogels based on natural polymers. *Hydrogels Based Nat. Polym. 2020,* 151–172. https://doi.org/10.1016/B978-0-12-816421-1.00006-9

Kurusu, R. S., & Demarquette, N. R., 2018. "Surface modification to control the water wettability of electrospun mats." *Int. Mater. Rev. 64(5),* 249–287. https://doi.org/10.1080/09506608.2018.1484577

López de Armentia Hernández, S., 2022. "Development of nanomaterial-based scaffolds for bone tissue regenaration." *Gels 9(2),* 100. https://doi.org/10.3390/gels9020100

Nancy, G. A., Kalpana, R., & Nandhini, S., 2022. "A study on pressure ulcer: influencing factors and diagnostic techniques." *The International Journal of Lower Extremity Wounds 21(3),* 254–263. https://doi.org/10.1177/15347346221081603

Nguyen, S., Nguyen, H., & Truong, K., 2020. "Comparative cytotoxic effects of methanol, ethanol and DMSO on human cancer cell lines." *Biomedical Research and Therapy 7(7),* 3855-3859. https://doi.org/10.15419/bmrat.v7i7.614

Niculescu, A. G., & Grumezescu, A. M., 2022. "An up-to-date review of biomaterials application in wound management." *Polymers 14(3),* 421. https://doi.org/10.3390/polym14030421

Pellis, A., Guebitz, G. M., & Nyanhongo, G. S., 2022. "Chitosan: Sources, processing and modification techniques." *Gels 8(7),* 393. https://doi.org/10.3390/gels8070393

Raja, P. B., Munusamy, K. R., Perumal, V., & Ibrahim, M. N. M., 2022. "Characterization of nanomaterial used in nanobioremediation." *Nano-Bioremediation: Fundamentals and Applications 2022*, 57–83. https://doi.org/10.1016/B978-0-12-823962-9.00037-4

Rianjanu, A., Kusumaatmaja, A., Suyono, E. A., & Triyana, K., 2018. "Solvent vapor treatment improves mechanical strength of electrospun polyvinyl alcohol

nanofibers." *Heliyon 4(4),* e00592. https://doi.org/10.1016/j.heliyon.2018.e00592

Sanjarnia, P., Picchio, M. L., Polegre Solis, A. N., Schuhladen, K., Fliss, P. M., Politakos, N., Metterhausen, L., Calderón, M., & Osorio-Blanco, E. R., 2024. "Bringing innovative wound care polymer materials to the market: Challenges, developments, and new trends." *Adv. Drug Delivery Rev. 207,* 115217. https://doi.org/10.1016/j.addr.2024.115217

Shah, A., Ali Buabeid, M., Arafa, E. A., Hussain, I., Li, L., & Murtaza, G., 2019. "The wound healing and antibacterial potential of triple-component nanocomposite (chitosan-silver-sericin) films loaded with moxifloxacin." *Int. J. Pharm. 564*, 22–38. https://doi.org/10.1016/j.ijpharm.2019.04.046

Sirin, S., Cetiner, S., & Sarac, A. S., 2013. "Polymer nanofibers via electrospinning: Factors affecting nanofiber quality." *Kahramanmaras Sutcu Imam University Journal of Engineering Sciences 16(2), 1-12*.

Toriello, M., Afsari, M., Shon, H. K., & Tijing, L. D., 2020. "Progress on the fabrication and application of electrospun nanofiber composites." *Membranes 10(9),* 204. https://doi.org/10.3390/membranes10090204

Waqar, M. A., Mubarak, N., Khan, A. M., Shaheen, F., Mustafa, M. A., & Riaz, T., 2024. "Recent advances in polymers, preparation techniques, applications and future perspectives of hydrogels." *Int. J. Polym. Mater. Polym. Biomater. 74(4),* 265–284. https://doi.org/10.1080/00914037.2024.2335163

Xu, Y., Liu, K., Yang, Y., Kim, M.-S., Lee, C.-H., Zhang, R., Xu, T., Choi, S.-E., & Si, C., 2023. "Hemicellulose-based hydrogels for advanced applications." *Frontiers in Bioengineering and Biotechnology 10,* 1110004. https://doi.org/10.3389/fbioe.2022.1110004

Yang, Y., Du, Y., Zhang, J., Zhang, H., & Guo, B., 2022. "Structural and functional design of electrospun nanofibers for hemostasis and wound healing." *Adv. Fiber Mater. 4,* 1027–1057. https://doi.org/10.1007/s42765-022-00178-z

Zhang, H., Chen, C., Zhang, H., Chen, G., Wang, Y., & Zhao, Y., 2021. "Janus medical sponge dressings with anisotropic wettability for wound healing." *Applied Materials Today, 23,* 101068. https://doi.org/10.1016/j.apmt.2021.101068

Zhang, H., Xu, Y., Lei, Y., Wen, X., & Liang, J., 2022. "Tourmaline nanoparticles modifying hemostatic property of chitosan/polyvinyl alcohol hydrogels." *Mater. Lett. 324,* 132718. https://doi.org/10.1016/j.matlet.2022.132718